Review of "How ice apron loss and permafrost degradation promote the Platteikogel rock slide: A thermo-mechanical reconstruction"

Response to RC2, Florence Magnin.

Dear Reviewer,

We sincerely thank you for your dedicated time and effort in reviewing the manuscripts.

Our answers and comments to your observations are found below your comments.

Major remarks

1) Characterization of the gravitational event: similarly to the first reviewer, I would suggest reconsidering the designation of the event, as it does not strictly correspond to a rock slide, and ensuring consistent terminology throughout the manuscript. « Rock slope failure » is neutral but « rock fall » is also frequently used for such volumes. And a minor remark : would the title be more precise with « promoted » instead of « promote ». At first sight, the combination of present tense + « rock slide » let me thought that it was an active rockwall deformation, not a past and sudden vent.

We adapted the landslide terminology according to your suggestions and those of Reviewer 1. Now, the more general term of rock slope failure is used throughout the publication, leaving aside process kinematics. "Rock slide" was substituted with "rock slope failure" throughout the manuscript. Moreover, a discussion paragraph about the process classification was added (see response to reviewer 1).

Moreover, we adapted the title by switching to the new terminology, and from the present to the past form of the verb "promote": *How ice apron loss and permafrost degradation promoted the Platteikogel rock slope failure: A thermo-mechanical reconstruction*

We clearly describe a past event, and therefore, the use of the present tense is not appropriate. Thank you for the remark.

2) The consideration of hydrological processes is frequently mentioned in the manuscript; however, it is not investigated at the same level as the thermal and mechanical processes. Its treatment remains more arbitrary and is not calibrated as the thermal and mechanical processes. It is also unclear how the approach for testing the water-related pressure was defined (determination of a hydraulic head of 30 m). I would therefore recommend clarifying this difference in approach in order to better structure the conclusions and to more clearly distinguish the respective contributions of the different methods and approaches.

Our study aims to address promoting drivers for rock slope failure by mechanically investigating the rock slope's response to observed rockfalls (Sect. 2), permafrost warming (Sect. 3.1), and other mechanisms, as stated in the research questions. A highly mechanically relevant but hard to constrain other mechanisms is hydrostatic pressure within rock slopes, which was not investigated in the same detail as rockfalls and permafrost prior to the mechanical modeling study. Rather than recreating actual groundwater conditions, we emphasized illustrating the mechanical consequences of ponded subsurface water within the modeling study via a simplified approach by assigning a hydrostatic water column to defined areas within the rock mass.

In *Section 3.1 The mechanical implications of ice apron loss*, we draw the conceptual basis for our mechanical modeling setup by explaining the interwovenness of permafrost, hydrogeology (water pressure mentioned for the first time), and rock slope mechanics.

With Section 3.2.4 explaining the scenario implementation for the mechanical simulation study, we now specify the implementation, goal, and limits of hydrostatic pressure application. **We made the following paragraph extension (bold),** for completeness; the introductory paragraph was copy-pasted:

S2 Transient buildup of hydrostatic pressure

The buildup of hydrostatic pressure within permafrost rock is a central trigger for releasing permafrost rock slope failure (Gruber et al., 2007; Fischer et al., 2010; Pfluger et al., 2025). Although observations and measurements of permafrost hydrogeology in rock slopes are scarce and typically site specific, a field study based on decadal observation suggests plausible values for transient water columns in fracture systems of several decameters upon peak snow melt or rainwater infiltration periods (Scandroglio et al., 2025; back calculation from water discharge measured at fracture outlet). In addition, piezometric heads of more than 10 m were recorded in boreholes within fractured rock in permafrost (Offer et al., 2025) and sporadic permafrost (Aspaas et al., 2026). Moreover, failure scarps of larger failures often exhibit wet areas, observed directly after detachment, which point to locally ponded water within the rock mass short before sudden-failure conditions (i.e., (Fluchthorn, Austria, 2023 event, Krautblatter et al., 2024; Piz Scerscen, Switzerland, 2024 event, PERMOS, 2024).

With this scenario, we test the mechanical response to applied hydrostatic pressure equivalent to a 30 m water column, representing hydrogeological conditions upon peak surface water infiltration - compare to reported hydrostatic heads of 27 ± 6 m during average snowmelt and 40 ± 10 m for extreme events (Scandroglio et al., 2025). The pressurized zone is assigned a lateral width of 30 m and applied to different regions of the rock mass. Throughout the mechanical cycling, static water pressure is applied within discontinuities only, exerting normal stress on joint walls, while pore pressure within blocks is neglected.

Temporal hydrogeological evolution is not explicitly modeled. Instead, spatially variable pressurized zones are used to represent conceptually inferred, locally ponded groundwater conditions within permafrost rock slopes, potentially promoted by channelized flow along fractures (Hasler et al., 2011; Magnin et al., 2021).

Unlike the analysis of observed rockfalls (Sect. 2) and permafrost warming (Sect. 3.1), changing groundwater conditions were not directly captured within the scope of this study, but their implications were inferred conceptually.

This setup does not aim to reproduce actual groundwater conditions but isolates the mechanical effect of water pressure, emphasizing the sensitivity of slope stability to the spatial availability of water within the rock mass.

In addition, we have performed mechanical simulations with the hydraulic heads of 20 and 10 m, respectively. While the highest mechanical impact was clearly associated with the peak water infiltration scenario, as demonstrated with the example of a hydraulic head of 30m, lower heads affect slope mechanics in minor magnitudes (see Figures attached at the end of this document). Both the location of applied pressure (Fig. 11 a,b,c) and the absolute hydraulic head affect the mechanical response.

3) Simulations consider various scenarios such as thermal evolution, hydrological forcings and changes in mechanical properties that are treated independently following initial mechanical conditions with 2 possible setups. I found it somewhat challenging to clearly understand the different scenario combinations and the specific novelty each one brings to the understanding of rock slope failure predisposition and triggering mechanisms. While the overall approach is comprehensive, it is also relatively complex. **I would therefore suggest clarifying more explicitly the respective contribution of each scenario in comparison with the initial conceptual model.** I acknowledge that efforts have been made to make the results as clear and traceable as possible; however, in its current form, it remains difficult to clearly identify the actual contributions**. I believe greater clarity is needed regarding the a priori conceptual model and how the different simulations and process combinations either refine this model or allow the quantification of the underlying processes.**

The conceptual a priori model aims to draw the complexity of the system and to decipher individual factors that are relevant for rock slope destabilization. The conceptual model served as a basis to draw an abstracted, but robust framework for the mechanical modeling study conducted in the paper. As described with the derived conceptual model, which was used as an introduction to the mechanical modeling setup (Sect. 3.1, addressing singular and interwoven impacts), system feedbacks are highly interlinked. To simplify, we abstracted this to isolated scenarios, each one having a mechanical impact on slope stability.

I would therefore suggest clarifying more explicitly the respective contribution of each scenario in comparison with the initial conceptual model.

The answer to this statement is found in Figure 6b. It gives a compact overview of the individual mechanical simulation scenarios and how they are implemented. By viewing this, it should be clear that scenarios represent quasi-static images of the rock slope for specified external forcings, rather than demonstrating interlinked complex system feedbacks (as addressed by the conceptual model). The mechanical simulations capture only glimpses of possible rock slope states. Yet adding up S1, S2, and S3, we suggest that we covered the relevant drivers for rock slope destabilization under the given environmental conditions.

To clarify, we added the following statement under Methods Section 3.2.4: Scenarios and implementation:

Based on considerations of possible promoting factors or triggers (Section 3.2.1, Fig. 5), we examine the following scenarios, aiming to investigate the mechanical response to a changing cryosphere. These scenarios represent quasi-static realizations of the rock slope under specific states or external forcings (Fig. 6b) and therefore illustrate mechanical system responses to isolated effects rather than complex interwoven system dynamics.

… **quantification of the underlying processes.**

We have now made attempts to quantify the underlying processes relevant to driving the rock slope failure at Platteikogel, according to our mechanical modeling results**. The following paragraph and figure were added to the "Results" section:**

To quantify the mechanical impact of the individual processes, we compare scenario results by using the modeled absolute x-displacement recorded at the end of cycling 30000 mechanical time steps for the specified monitoring location as the benchmark metric (see displacement functions in the figures). The comparison in Figure 13 demonstrates that hydrostatic pressure (as modeled here) had the most pronounced impact on the kinematic response of the rock

slope. Permafrost, as modeled with the implementation of the temperature-dependent shear criterion, had no impact on the destabilization process. The impact of rockfalls depends on the structural model setup: While setup A showed minor effects, setup B exhibited x-displacements comparable to those suggested by hydrostatic pressure (cf. S3: a and b in Figure 13). Small block sizes facilitated shearing along many substructures and favoured locally the sliding of neighbouring blocks affected by the void at the post-rockfall state. In general, a smaller block size (setup B) led to lower total x-displacement at the monitoring location, compared to a larger block model with a defined shear basal shear plane (setup A). Within a single setup, however, displacement patterns remain internally comparable between scenarios. Both model setups indicate that at higher pre-failure shear strength (base model S1), the kinematic rock slope response is less susceptible to hydrostatic pressure applied and rockfalls.

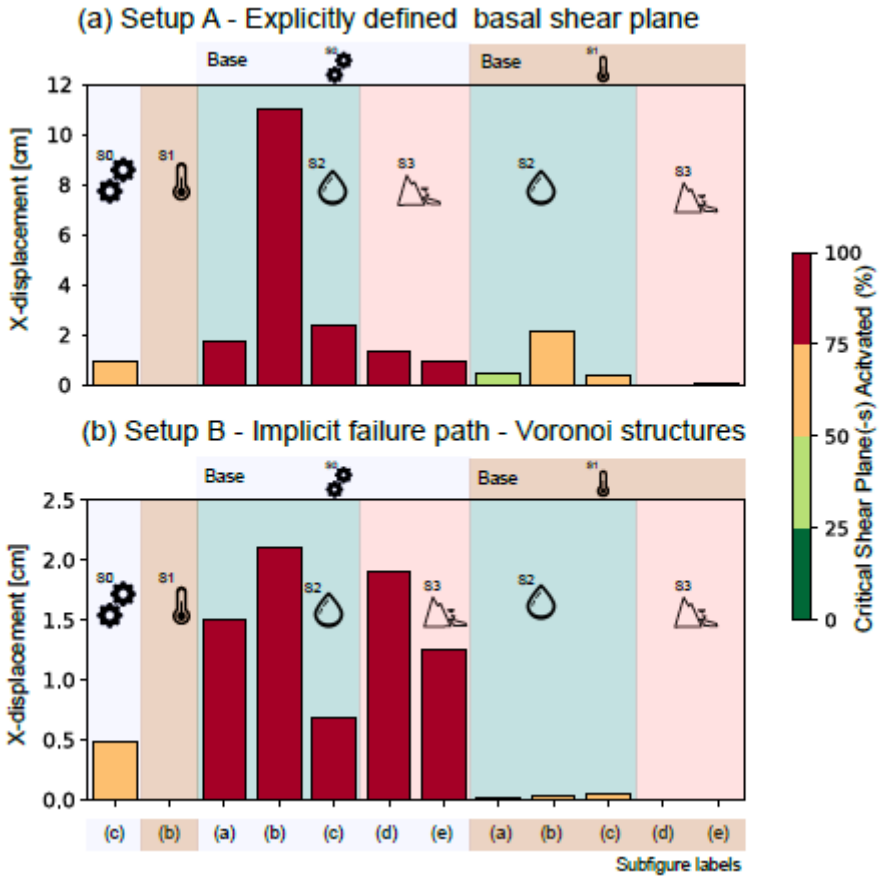

Figure 13. Compilation of results listed for each scenario shown for the structural model configuration of (a) setup A and (b) setup B. The bars display the absolute x-displacement at the end of cycling 30000 mechanical time steps for the location of the monitoring point shown in the reference figures. Results stem from individual simulations shown for (a) in Figures 9–12 and for (b) in Figures A3–A6. The color scale indicates the relative share of the basal shear plane / critical shear planes that is activated at this model state. Note: In UDEC, “mechanical time steps” refer to numerical iterations. One model step corresponds to 0.00492 s (setup A) and 0.00342 s (setup B) of physical time, regardless of the individual scenarios simulated. Model steps scale linearly with time.

4) Following this previous comment, Figures 1 and 12 are somewhat similar and, in my interpretation, Figure 1 presents the a priori hypotheses, whereas Figure 12 corresponds to an enriched version of Figure 1 incorporating the modeling results. However, it remains difficult to clearly distinguish from Figure 12 which elements are firmly supported by the results and which remain more or less speculative after consideration of the modeling outcomes. I believe it would be useful to more clearly differentiate the results that are robustly established from those that merely maintain or confirm the initial a priori hypotheses within this conceptual model.

Figure 1 comprises both, the a priori hypothesis and the structure of the manuscript and methods used, indicating the iterative information flow (surface ice changes and rockfall mapping (Sect. 2) -> permafrost temperature (Sect 3.1) -> mechanical slope response (Sect. 3.2)). It gives a clear focus and direction to the paper, while reducing complexity. Therefore, we prefer to show it at the beginning of the manuscript to direct the reader.

We agree with your concerns about Figure 12. As it was presented, it is not visible what results stem from the mechanical modeling study and what results are of a more conceptual/theoretical nature. **We renewed the Figure accordingly, presenting (a) the progressive failure theory and (b) highlighting the results from our simulations**:

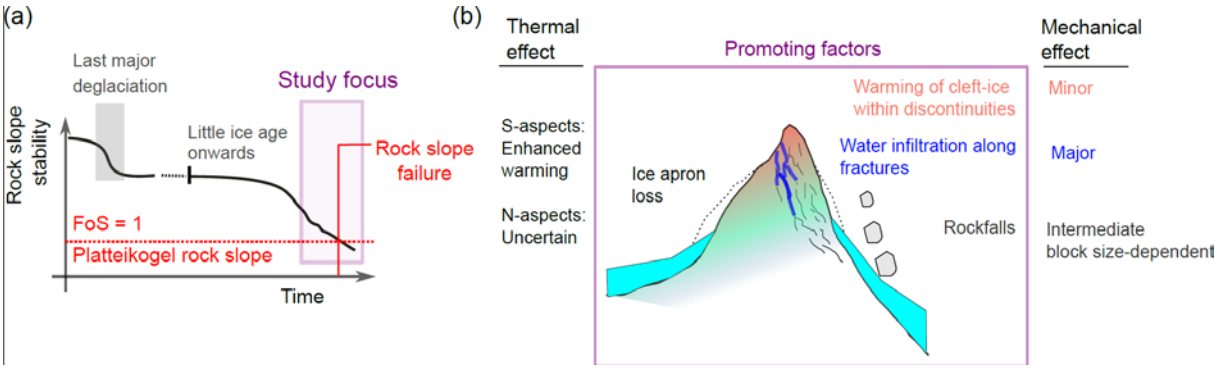

Figure 12. (a) Conceptually inferred stability function of the Platteikogel rock slope, highlighting the non-linear influence during the peri-paraglacial transition. (b) Dominant promoting factors investigated in this study that are relevant in the period shortly before failure. Results from the thermal and mechanical simulations are included to illustrate the corresponding impact.

The **paragraph was rewritten accordingly:**

The concept of progressive failure mechanism and the promotion of the Platteikogel rock slope failure is explained theoretically (Fig. 12}a) and on the basis of our simulation results (Fig. 12}b) : Cold permafrost since the Little Ice Age stabilizes the slope by adding cohesion through ice in fractures, and suppressing crack propagation (Krautblatter et al., 2015). However, in recent decades, ice apron loss and warming air temperatures have accelerated permafrost warming. The observed rockfall activity, together with ice apron loss, modified the topography. Consequently, elastic rock mass adaptation leads to widening of joints (Leith et al., 2013; Grämiger et al., 2017). Ice apron loss, joint widening, and heterogeneous permafrost conditions, which are typically found in complex topographic terrain (Nötzli et al., 2007), favour the infiltration of water into the rock slope and therefore hydrostatic pressure buildup within stability-relevant (scenario S2). Given sufficient accumulated pre-failure damage (i.e. base model S0), the rock slope is prone to failure upon hydrostatic pressure buildup during peak water infiltration (snowmelt/rainfall events, S2) or as a response to rockfalls (S3, setup B: small block-size model). Yet, shear strength degradation as a result of permafrost warming (S1) had a

minor impact on the destabilization (Fig. 12b). The implications of permafrost warming and strength degradation are discussed in the following section in detail.

5) I have been somewhat confused through the manuscript, as the failure depths (mean/max) are not clearly specified and the basal shear strength does not correspond to the V/A ratio. I believe this point should be clarified to ensure that the initial assumptions, as well as the contributions and limitations of the results, are more easily understandable and identifiable.

We added the estimated depth of the shear plane to Table 1, which is shown at the beginning of the site characterisation.

Estimated average depth of basal shear plane 20 m (range: 15–25 m);
Moreover, we reference the numbers to the corresponding figure: The location and shape of the basal shear plane are shown in the profile in Figure 6a.

V/A ratio: Here, confusion likely occurred between the volume of the detachment area (source area only) and the total affected area (detachment area including the deposition area), which is typically used to calculate the V/A ratio (mobility metric of landslides). To clarify, we included

Affected total area including deposits A 48,000 m^2 .

6) Despite the very high quality and richness of the figures, they are sometimes difficult to read due to the large amount of detail, with text that is occasionally too small.

We tackled this concern by modifying the following figures to increase readability via enlarging sizes/text/colorscales or rearranging material: Fig. 2,5,6b,9, A3. Figure 11 and A5 were split from one figure with 10 subfigures into two figures with 5 subfigures, respectively.

Minor remarks

L41 : I would use « multi-method approach » rather than « cross-disciplinary »
Corrected.

L67-75: how was this measured?
Via structural analysis of two rock outcrops (shown in Figure A1; methods are briefly explained in the caption): Structural analysis of two rock outcrops in proximity to the detachment area. In total, 11339 planes were reconstructed and analyzed using the FACET plugin in Cloud Compare software (Dewez et al., 2016). Parameters for FACET plugin: Fusion algorithm Kd-tree, max-anlge 20, max relative distance 1.00.

We added the following to Figure A1 in the text: (Figure A1 - analysis of rock outcrops) to clarify.

L90-99: how are all these changes calculated?

It is referenced in the Figure. The caption clarifies how "The spatio-temporal surface ice changes (d-f) and rockfall inventory (g-i) were processed following the approach for multi-temporal quantification of surface changes described in the supplement of Barbosa et al. (2024)."

L105 and following: a few words decribing the Cryogrid (coding, physics…) would be useful

We added the following statement as an introduction. Central references are already given in the first manuscript version.

With Cryogrid 2D, the subsurface temperature field is calculated by solving the heat diffusion equation following Fourier's law of heat conduction according to defined material- and temperature-dependent parameters. The finite element solver MILAMIN package \citep{Dabrowski.2008} was employed to numerically solve complex geometries on unstructured grids, based on specified boundary conditions and the imposed temperature forcing along the model topography. Time discretisation follows a finite-difference backward Euler scheme. A detailed description of the CryoGrid 2D model is provided by \cite{Myhra.2017}. Here, we use the Cryogrid 2D version as applied by \cite{Czekirda.2023}. The modeling strategy follows their approach and is outlined below.

L110: Any performance metrics beyond the visual in Figure A2 for the calibration?

Model performance was well validated in other papers (see cited literature: Myhra et al., 2017, 2019; Czekirda et al.,2023). Moreover, we used same rock parameters as in the studies of Myhra et al. (2017, 2019), as the rock type is very similar (gneiss). In addition to what is shown in Fig. A2a we computed calibrations to measured Matterhorn borehole data for varying pairs of thermal conductivity using a single column model: We tested variations of k = [2,3] W K-1m-1 and cv = [1.5,2.0,2.5,3.0] 10^6 m-3 K-1. Best-fit for the depth of shear plane (15-25 m) with the pair of thermal conductivity k, and volumetric heat capacity of cv is shown in Fig. A2a and was used throughout the simulation study.

L145: the Equation neglects the effect of permafrost on the snow-covered surface as the RST generally falls well < 0°C below snow under permafrost conditions, especially on the NW aspect where permafrost is cold. This limitation deserves to be taken into consideration in some ways.

This is a valid point. Like all the other equations used here (Eqs. 1–4), the model forcing is represented by a one-way transfer function: atmospheric forcings are applied to the rock surface. Consequently, temperatures at the base of the snow cover are treated as being driven solely by the climate (top-down), while the influence of underlying permafrost (bottom-up) is

neglected at the model boundary, where forcings are applied. This simplification may lead to underestimating the effect of permafrost on the bottom of snow temperatures (bottom-up), particularly under cold, NW-facing permafrost. Our model approach did not tackle this issue. We implemented the effect of snow cover on RST via an empirical transfer function using nF factors (Smith and Riseborough, 2002) and air temperature as variables. Due to unknowns about local heat-fluxes and spatial and temporal uncertaintiy in snow cover, we adopted this rather simplified approch. **We made the following changes**:

Following Czekirda et al. (2023), we used the slope of the profile to assess the nF-factors ranging from 0.5 for slope < 30° to 1 for slope > 60° along the profile topography and calculated RST below the snow cover using the empirical transfer function (see Fig. SM3).

We address the issue you raised separately in the Discussion section "Representation and limits of thermal processes in CryoGrid 2D". The following paragraph was added:

The climatic model forcing (RSTs) was computed by one-way transfer functions (Eqs. 1-4). Consequently, temperatures at the base of the snow cover or ice aprons are treated as being driven solely by the climate (top-down), while the influence of underlying permafrost (bottom-up) is neglected at the model boundary, where the forcing is applied. This simplification may lead to underestimating the effect of permafrost on the bottom of snow temperatures, particularly under cold, NW-facing permafrost, an issue that was not resolved within this study.

L167: the meaning of TIAS is not detailed.

We inserted the following definition right above the presented formula:

TIAS refers to the Temperature at the Ice Apron Surface specified for a location of 0.1 m below the current ice surface (analogous to the standard depth specified for RST measurements).

L 193: I didn't get what these 100 simulations correspond to. This deserves clarification.

We added for clarification:

Starting from the initialized state in 1900, we ran 100 individual simulations until 2024 in order to account for uncertainties through the use of temperature transfer functions. Each simulation was forced with RST calculated on basis of randomly sampled offset parameters within specified ranges: Eq. 1: $x \in [-0.1, 0.1]$; Eq. 2: $SO\_N\,W \in [-1, +1]$, $SO\_SE \in [+2, +4]$ °C; Eq. 3: $H\_ice \in [1, 9]$ m; Eq. 4: $nF \in [+0.4, +0.6]$.

L 259: I get confused by « varying model geometry ». If I look at figure 6, A & B are two different rock structure/jointing systems setups, right? Could the sentence be more precise? In my opinion « geometry » could also refers to the topography, rock/ice distribution, and varying sounds like a dynamical parameters, while it seems 2 different setups.

We agree that the wording "varying model geometry" may be misleading. In this context, we refer to two distinct structural model configurations - two different modes representing structural geology on different degrees of detail / and emphasizing abstraction of failure planes.

We substituted "model geometry" with "structural model configuration".

L285: how the value of 30 m for the hydraulic head was decided?

Please refer to the answer to (2) in the major remarks above.

L308: low rather than « cold » temperature.

Corrected.

L 314: why 20 m depth? Is it the failure depth? Basal shear plane?

It is the average depth of the failure plane (Shown in Figure 6b, and specified in Table 1.)

L320: « extrusion-like form » is not clear to me

The temperature profile indicates a flip in temperature progression from a local depression (1980) towards a local peak (2023). Wording rephrased.

L322: « (« is missing before « Fig.8) »

Corrected.

L344: permafrost temperature is lowest rather than « coldest »

Corrected.

L405: for this study, the concept of peri-paraglacial would be more appropriate

Wording adapted from “during the transition from paraglacial to periglacial conditions”

L440: fatigue

Corrected.

L 520: unclear sentence, any word missin?

Rephrased to: Degrading ice aprons feature geomorphic change by enhancing frost-weathering activity and water infiltration into rock slopes, which in turn facilitates the generation of rock slope failures. Atmospheric recoupling, hydrostatic pressure buildup, and stress alterations from ice apron loss and rockfalls drive progressive failure, as demonstrated by the mechanical simulation.

L525: what would be « sufficient information »?

Rephrased to: Given the major ice apron loss and structural predisposition at the Platteikogel, similar rock slope failures may be anticipated if kinematic monitoring data are available.

Table 1: any idea of the max mean/depth? Looking at the volume/surface area it seems that the event is really shallow and this has strong implications for the thermal models that may not be realistic at all at shallow depths. And in Figure A2 a there is a « depth of basal shear plane ». Is it between 15 and 25 m? I a ma bit confused as this information is not clearly reported.

Yes, it is between 15 and 25 m. The answer to this remark is found at # 5 under major remarks.

Fig. 7: I didn’t get why is the reference line -3°C?

It shall serve as a visual reference to better compare changes between subfigures (b,d). But yes, it was kind of dominantly presented and was removed now, as the subfigures contain grids anyway.

Fig. 8: what is the dark-brown color?

It is shown in the color scale: temperature range between 0.01 and 0.1 °C.

Figures served to answer questions raised but not included in the manuscript.

Mechanical sensitivity to varying hydrostatic pressure heads (a) 30 m, (b) 20 m, and (c) 10 m.

(a) 30 m (same result and location (central) as shown in Figure 11b)

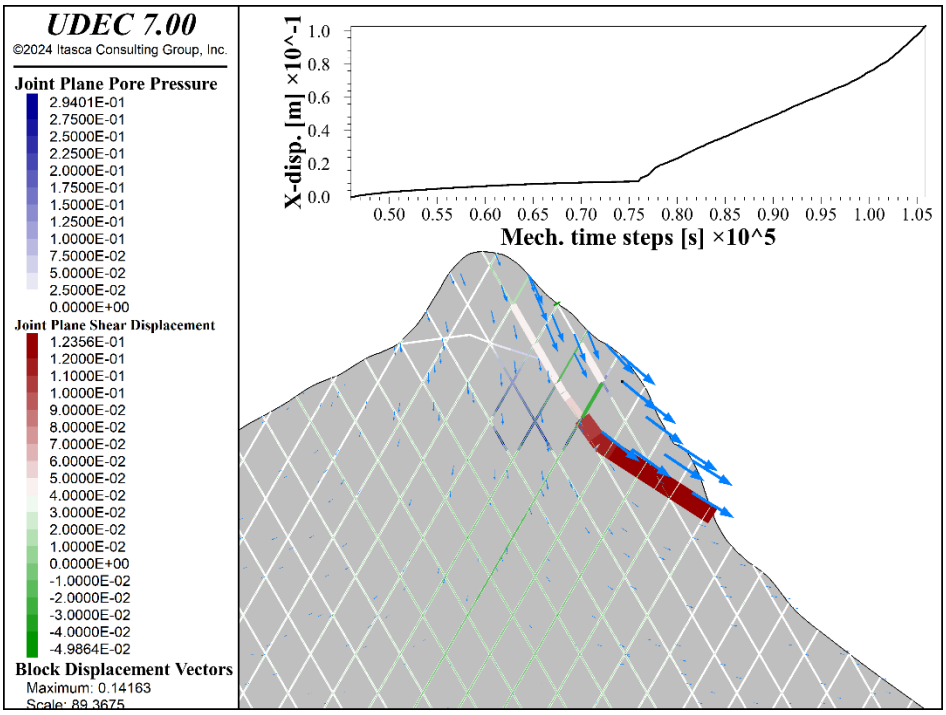

(b) 20 m.

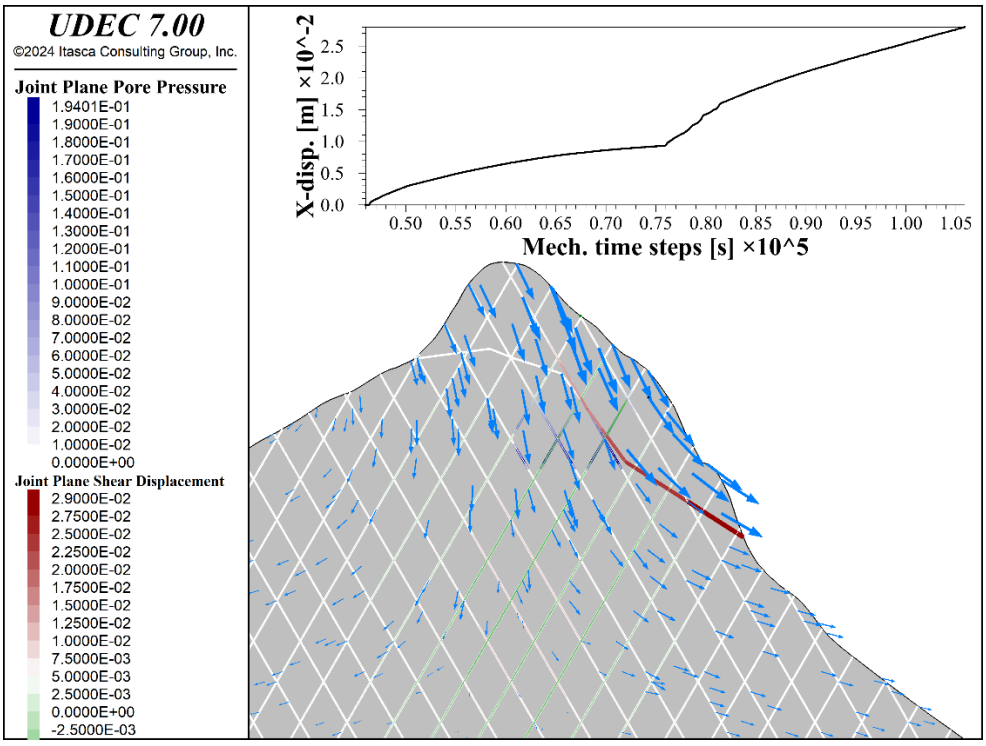

(c) 10 m.

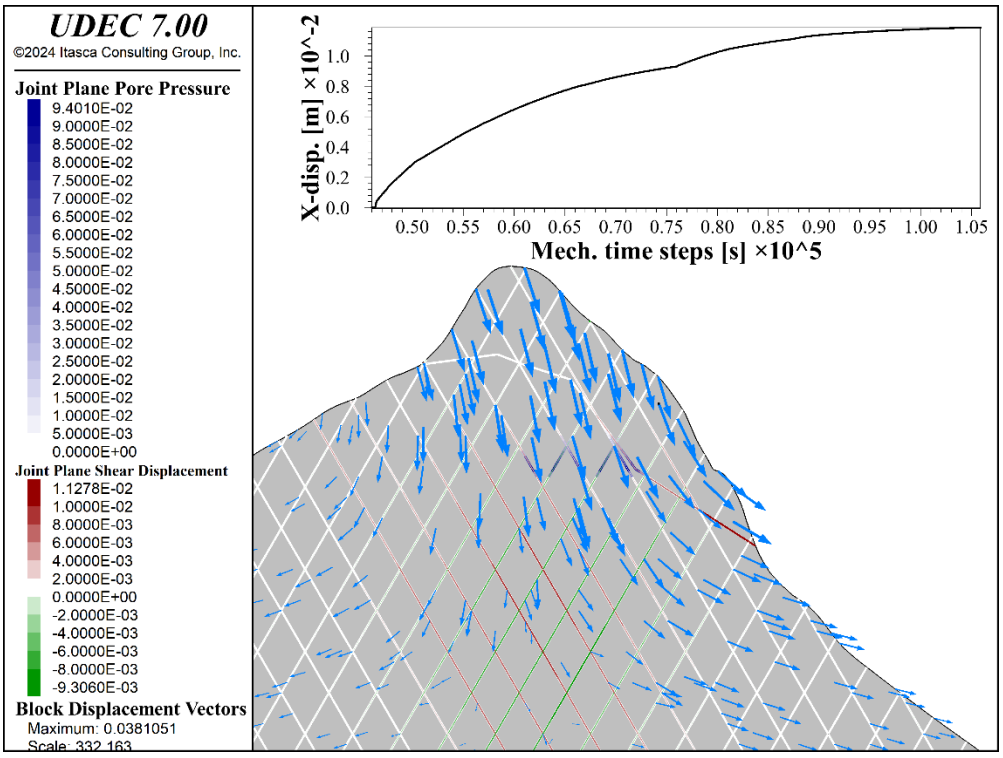
UDEC 7.00
©2024 Itasca Consulting Group, Inc.
Joint Plane Pore Pressure
9.4010E-02
9.0000E-02
8.5000E-02
8.0000E-02
7.5000E-02
7.0000E-02
6.5000E-02
6.0000E-02
5.5000E-02
5.0000E-02
4.5000E-02
4.0000E-02
3.5000E-02
3.0000E-02
2.5000E-02
2.0000E-02
1.5000E-02
1.0000E-02
5.0000E-03
0.0000E+00
Joint Plane Shear Displacement
1.1278E-02
1.0000E-02
8.0000E-03
6.0000E-03
4.0000E-03
2.0000E-03
0.0000E+00
-2.0000E-03
-4.0000E-03
-6.0000E-03
-8.0000E-03
-9.3060E-03
Block Displacement Vectors
Maximum: 0.0381051
Scale: 332.163
X-disp. [m] ×10^-2
1.0
0.8
0.6
0.4
0.2
0.0
0.50 0.55 0.60 0.65 0.70 0.75 0.80 0.85 0.90 0.95 1.00 1.05
Mech. time steps [s] ×10^5